

**Original
Article**

USE OF ELECTRONIC PORTAL IMAGE DEVICE IN SOME QA TESTS

N. A. El-Sherbiny¹, M. A. AbouZeid², M. A. Ellaithy³ and W. F. Mohamed⁴

¹Department of Oncology and Nuclear Medicine, Faculty of Medicine, Cairo University, ²Department of Physics, Faculty of Science, Mansoura University, ³Department of Oncology, ⁴Nuclear Medicine, Department Mansoura University Hospital.

ABSTRACT

Introduction: In the present study a method to investigate light and radiation field congruence utilizing an amorphous silicon electronic portal imaging device (EPID) was developed. An alternative method for routine dynamic multi-leaf collimator (DMLC) quality assurance (QA) using EPID was also described.

Materials and Methods: This study employed an amorphous silicon (aSi) EPID, the associated EPI software and a diamond-shaped template. The collimator jaws of the linac (Elekta iViewGT) were aligned such that the light field fell directly on the corners of the diamond. A radiation detection algorithm within the EPI software determined the extent of the radiation field. The light and radiation field congruence was evaluated by comparing the vertices of the diamond reference structure to the detected radiation field. In addition, the digital jaw settings were recorded and later compared to the light field detected on Kodak x-omat films and EPIs. In this study an alternative method for routine dynamic multi-leaf collimator (DMLC) quality assurance (QA) using (EPID) was described. This QA was done by producing a pattern of five 0.5-cm bands 5-cm apart and performing a visual spot-check for dose peak location, dose peak values, interband distance and band gaps measured at Full Width at Half-Maximum (FWHM) of the test pattern for this QA experiment. An aSi EPID and films are used for the DMLC QA to test the practicality and efficacy of EPID vis film.

Results: Light radiation field congruence tests with films and EPIs were comparable, yielding a difference of less than 1.2 mm, well within the allowed 2-mm tolerance. A disparity was observed in the magnitude of the detected light field. The X and Y dimensions of the light field measured with film differed by less than or equal to 1.6 mm from the digital collimator settings, whereas the values extracted from the EPIs differed by up to 1.8 mm. The FWHM of the multi-leaf collimator (MLC) obtained by the EPID is 6.34 mm, which is slightly higher than the 6.18 mm for the film. The lowest dose at the valley is significantly lower for the EPID than for the film. The dose peak value of the EPID is found to be 97.9 with standard deviation of ± 1.59 and the dose peak value of film is found to be 96.5 with standard deviation of ± 2.41 , respectively. Film and EPID track the distance between peaks with a mean of 49.8 and 49.53 mm and standard deviation of ± 0.3 and ± 1.02 mm, respectively. EPID is able to track the location of individual dose peaks for all the leaf pairs consistently to a standard deviation of ± 0.12 to ± 0.47 mm, slightly better than that of ± 1.00 to ± 1.26 mm for the film.

Conclusion: EPIs were found to be a quick and reliable alternative to film for qualitative and relative analyses. Also EPID is as good as the film in resolving the band pattern of the DMLC test field. Although the resolution of the EPID is lower than that of the film, it is high enough to faithfully reproduce the band pattern without significant distortion. Since EPID images can be acquired, analyzed and stored much more conveniently than film, EPID is a good alternative to film for routine DMLC QA.

Key Words: Electronic portal image device, dynamic multileaf collimator quality assurance, light and radiation co-incident.

Corresponding Author: Walaa Fathy, **E-mail:** wha818@yahoo.com.

INTRODUCTION

As radiation oncology facilities begin to clinically implement intensity modulated radiation therapy (IMRT), the need to develop the appropriate quality assurance (QA) tests for geometric and dosimetric plan verification becomes essential. Several authors have suggested the use of electronic portal imaging devices (EPIDs) to facilitate this procedure.^{1,2}

Recent developments in aSi EPID have made it the device of choice for this application: Its imaging speed

can be as high as 10 frames per second and the detector has a linear response as a charge accumulation device; therefore, dose integration can be faithfully performed by the frame averaging³ Munro et al. also demonstrate that aSi EPID does not suffer from the glare phenomenon associated with camera-based EPIDs⁴.

Two different approaches have been developed for QA of MLC or IMRT treatment using EPIDs. The first

approach uses EPIDs to verify the leaf position⁵ or track the leaf trajectory⁶. This approach generally requires a complicated edge detection algorithm; for IMRT QA, faster imaging (or sampling) speed is also needed to catch up with the leaf motion. In Samant's study⁵, an Elekta iViewGT EPID with an imaging speed of 3.5 frames per second was successfully used to track leaves moving at the speed of 0.7 cm/s. Recent developments in aSi EPID have made it the device of choice for this application: Its imaging speed can be as high as 10 frames per second and the detector has a linear response as a charge accumulation device; therefore, dose integration can be faithfully performed by the frame averaging³. Munro et al.¹¹ also demonstrate that this EPID does not suffer from the glare phenomenon associated with camera-based EPIDs.⁴

Two different approaches have been developed for QA of MLC or IMRT treatment using EPIDs. The first approach uses EPIDs to verify the leaf position⁶ or track the leaf trajectory⁶. This approach generally requires a complicated edge detection algorithm; for IMRT QA, faster imaging (or sampling) speed is also needed to catch up with the leaf motion. In Samant's study⁵, an Elekta iViewGT EPID with an imaging speed of 3.5 frames per second was successfully used to track leaves moving at the speed of 0.7 cm/s.

Instead of tracking the leaf motion, Others^{3,7,8} have used an EPID to measure the "delivered" integral dose or fluence profile. This approach can also be applied to IMRT using non-sliding-window techniques, e.g., physical compensators, multiple aperture fields, or wedges and this is less restricted by the imaging speed and is less sensitive to noise. J.Chang et al.⁷ indicated that ~1 frame/s is fast enough for reconstructing the delivered profile for Varian DMLC system with a maximum leaf speed of 2 cm/s. J.Chang also concluded in another study³ that there is essentially no sampling error for aSi EPID, except for the dose missed during reset of every 64 frames.

Intensity-modulated radiotherapy (IMRT) using the sliding window technique^{9,10} requires continuous leaf motion during dose delivery; the actual dose delivered depends very much on how accurately the motion of the dynamic multi-leaf collimator (DMLC) duplicates the pattern required by the optimized treatment plan. A stringent QA program is hence required for making sure that leaf motion is accurate, smooth and reproducible on every fraction of dose delivery.^{11,12} One of the QA procedures in IMRT is a machine QA on the DMLC leaf motion¹³, a film test of a standard DMLC leaf pattern is done. This DMLC leaf pattern consists of leaf pairs moving dynamically along the collimator x-axis, stopping momentarily each 5 cm of the way, giving five 0.5-cm bands exposure on film. The film is then visually inspected for leaf-pair alignment and uniformity of the band gaps between different leaf pairs. In case

of misalignment or band gap deviation, the film will then have to be scanned, digitized and analyzed using a film dosimetry program. Therefore if an electronic portal imaging device (EPID) (which saves on time and tedium because of its fast image archiving, retrieval and automated image analysis) has similar sensitivity for this QA procedure as film was investigated. To compete with the film, an EPID must be able to faithfully integrate the test IMRT pattern over time and to accurately convert the readings of integrated image to dose for QA analysis.

In this study, the feasibility of using an aSi EPID to replace film for our DMLC QA procedure was investigated. We analyze the sensitivity of both media by calculating the statistics of four measures—dose peak location, dose peak values, interband distance and band gaps measured at FWHM—of the test pattern for this QA procedure.

For this study, an accurate, efficient and reliable image-based quality assurance procedure utilizing an electronic portal imaging device is discussed. By substituting electronic portal images in place of film, the efficiency and the overall quality of this and other procedures can be improved.

MATERIALS AND METHODS

Film Dosimetry:

Ready Pack "Kodak X-Omat V Therapy Verification Film" (Inc., Rochester, NY, USA) were used in dosimetry measurements. All irradiated films were scanned using a computer controlled digital densitometer (FIPS PLUS laser scanner, PTW GmbH, Freiburg, Germany). Film optical density was calibrated to absolute dose using an irradiated calibration film.

FIPS PLUS laser densitometer:

It is a computer controlled digital densitometer (FIPS PLUS laser scanner, from PTW GmbH, Freiburg, Germany). It allows the evaluation of radiation therapy films, resulting in beam profiles, depth dose curves, isodose or 3D graphics. FIPS PLUS Scanner measures the optical density as it is done by conventional densitometer, i.e. the transmitted laser intensity is detected at a well-defined point on the film. The transmitted laser intensity is digitized with a resolution of 12 bit to ensure optimum accuracy of the measuring values. The maximum spatial resolution of the FIPS PLUS Scanner can vary between 0.2 mm and 0.34 mm.

Diamond structure:

Diamond shaped PMMA plate:

Diamond shape lead wire of a side length of 10 cm embedded in 1 cm thickness plate of PMMA and of area of 30 x 30 cm². The plate is manufactured for the check of light field coincidence with radiation field. The diamond template was created by fixing a wire square 10×10 cm² in dimension, rotated by 45°, onto the surface of a block

tray (see Figure 1-A). The central axis is denoted with a 1-cm cross wire into the center of the tray. The wires are made of a Sn/Pb alloy.

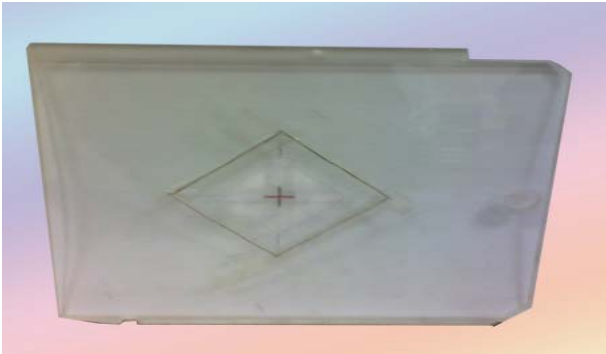


Figure 1-A: Diamond template constructed for light and radiation congruence test utilizing an EPID.

Amorphous Silicon (aSi) Detector Panel:

In this study, (EPID) amorphous silicon flat panel-type imager (Elekta iViewGT) was utilized. The detector panel is a PerkinElmer Amorphous Silicon (aSi) detector, which gives a resolution of 1024×1024 16-bit pixel image, with a detector panel size of $41 \times 41 \text{ cm}^2$ (approximately $26 \times 26 \text{ cm}^2$ at isocenter). The Elekta MLC linac is equipped with a 40 leaf pair MLC, each leaf having a width of 1 cm at the isocenter plane. The leaves have a maximum over travel across the beam axis of 12.5 cm. The maximum distance that one leaf can be extended beyond another on the same carriage is 14.5 cm. The data is read from the panel, through a data link into a frame grabber in the iViewGT™ computer. The detector comprises some layers: Aluminum Top Cover, Air Gap, Copper Plate, Graphite Layer, LANEX Fast™ Scintillator Plate, Attenuating Film and Photo Diode Array (Figure 1-B).

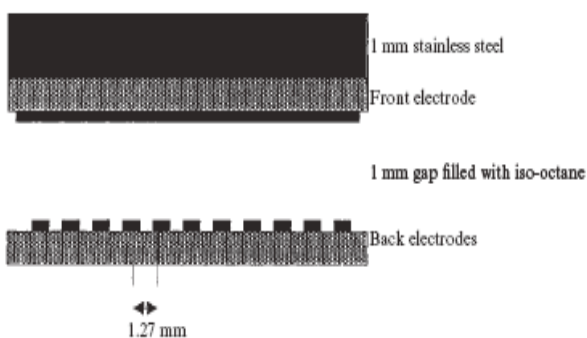


Figure 1-B: Cross-sectional representation of a liquid ion chamber array¹⁵.

I. Monitoring Light and Radiation Field Congruence using EPID:

To examine the light field and radiation field congruence using EPID a diamond-shaped structure are used. In this study the block tray were mounted on the Table of the linac on a sheet of Kodak X-Omat film (act as build up layer) that positioned 100 cm from the source over 5 cm of polymethylmetacrylate

(PMMA) slab phantom. All tests were performed with a gantry and collimator angle of 0° . A diamond shape is projected at isocenter with a vertex-to-vertex distance of approximately 14.5 cm. The EPID was positioned 156.5cm from the source, providing 0.5 mm pixel pitch at isocenter. Each asymmetric jaw of the linac was independently adjusted to intercept a vertex of the diamond. The field was irradiated with a dose of 10 MU.

The electronic portal images were acquired at low-energy (6 MV) x-ray beam. The digital setting for the X and Y jaws were recorded by EPID and later compared to the size of the detected light field. Although, at the same time the light field was determined by scribing the projected light field directly on the film jacket. Also, the digital collimator settings were recorded and later compared with the detected light field on the films and EPIs.

The electronic portal images (EPI) were analyzed with the associated EPI software. To analyze the images, a previously acquired image was stored as a reference. A diamond structure was drawn over the shadow cast by the block tray. The reference structure was aligned such that each of its sides overlaid the center of the diamond-shaped image. Latter EPIs were compared to the reference image by overlaying the corresponding reference structure over the center of the diamond on the newly acquired EPI (see Figure 2). The vertices of the reference structure represent the edge of the light field.



Figure 2-A: An example of a portal image acquired with the diamond template mounted on the treatment couch. (B) The image of the film acquired with the diamond template mounted on the treatment couch showing the difference between the reference structure and the radiation field, as defined by the EPI software and the film yields the light radiation congruence.

The light and radiation field congruence was determined by measuring the distance between each vertex of the reference structure and the detected radiation field. The evaluated light and radiation field congruence and the field size dimensions were compared with a film measurement. The light field size was compared to the absolute field size, as defined by the recorded digital collimator jaws.

The films were analyzed via visible inspection and considered the standard to compare the EPI results. The light field was defined as the distance between the two parallel marks drawn on the film. Similar to the EPIs, the light field size was compared with the field size as defined by the recorded digital collimator jaws. Data was analyzed using SPSS (Statistical Package for Social Sciences) version 10. Normally distributed data was presented as mean \pm SD. Student t-test was used to compare between two groups. $P < 0.05$ was considered to be statistically significant.

II. Determination of leaf position accuracy as a QA of dynamic multi-leaf collimator (DMLC) treatment:

A film test of a standard DMLC leaf pattern is done. As shown in (Figure 3), this DMLC leaf pattern consists of leaf pairs moving dynamically along the collimator x-axis, stopping momentarily each 5 cm of the way, giving five 0.5-cm bands exposure on film. The film is then visually inspected for leaf-pair alignment. The film then is scanned, digitized and analyzed using a film dosimetry program. The procedures are repeated with the electronic portal imaging device (EPID).

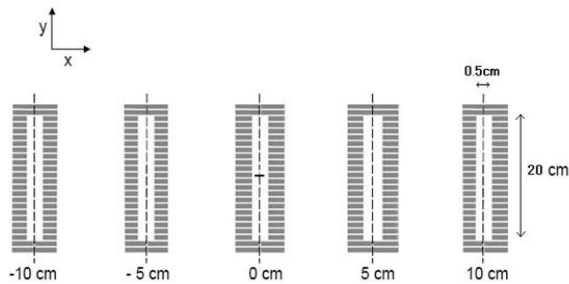


Figure 3: MLC field containing five $0.5 \times 20 \text{ cm}^2$ segments centered at positions $-10, -5, 0, 5, 10 \text{ cm}$, respectively. The cross shown at the center of segment 0 cm indicates the isocenter position.

The EPID was irradiated with a source to detector distance (SDD) of 156.5 cm , using the 6 MV , for 25 MU . To compare the performance of EPID device with film, a Kodak X-Omat V film and an aSi EPID were exposed using the standard DMLC test pattern and the film irradiated at source skin distance (SSD) = 100 cm with 1 cm PMMA as buildup. The EPID image was transformed to an integrated dose map by first converting the reading to dose using a calibration curve and then multiplied by the number of averaged frames. The EPID dose map was then back-projected to the central axis plane and compared to the film measurements which were scanned and converted to dose using a film dosimetry system.

In order to assess EPID's sensitivity vis film, the entire image of the test pattern were scanned and a statistical analysis of four important measures of the dose profile, namely dose peak location, dose peak values, interband distance and band gaps measured at FWHM were done. As shown in (Figure 4-A), there are five peaks in the test pattern, from which this measure can be derived to analyze the irradiated pattern. Pixel values of the EPID image were renormalized so that the average peak value of the EPID was the same as that of the film. The mean and the standard deviation of each measure of the test patterns are calculated and the results for the pattern obtained using the EPID to those obtained with the film are compared. We believe that any discrepancy in these parameters between the intended and actual dose delivery would cover many of mechanical DMLC problems. The results for the pattern obtained using the EPID to those obtained with the film were compared.

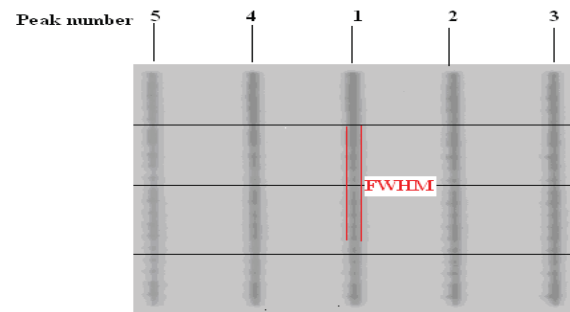


Figure 4-A: Images of the test pattern for simulated leaf problem, acquired using Kodak X Omat film with buildup 1 cm PMMA showing Dose profile parameters used in statistical analysis: dose peak location, dose values, inter-band distance and band gap at FWHM.

The leaves are mounted on a moving carriage, allowing for leaf movement across the central axis. The leaves move along straight lines. A uniform field was delivered dynamically by sweeping a prescribed $20.5 \times 20 \text{ cm}^2$ slit across the field with constant velocity. The jaws of the machine collimator were set to $20.5 \times 20 \text{ cm}^2$ in order to minimize transmission through the leaves outside the field.

The averaged image was converted to an integrated dose map following as previously mentioned. The EPID dose map was then back-projected to the central axis plane and was compared to the film measurements irradiated at source to skin distance (SSD) 100 cm with 1 cm PMMA buildup, scanned and converted to dose using the film dosimetry system.

RESULTS AND DISCUSSIONS

I. Monitoring Light and Radiation Field Congruence using EPID:

In this study, the errors were calculated. The deviations along each side of the projected field are summarized in (Table 1). In addition, results from

opposing field sizes were combined to yield the overall cross (ΔX) and in-plane (ΔY) deviations. Based on these results, no appreciable difference was observed in light and radiation field congruence between the conventional and the EPID-based technique discussed in this study (p -value >0.2) for ΔX and ΔY . A systematic error of less than or equal to 0.9 mm has been calculated for the cross and in-plane discrepancies. A comparison of the absolute field size as defined by the digital collimator jaw settings and the light field detected on the films and EPIDs is presented in (Table 2). Based on these results, the size of the detected light field differs depending on the QA technique utilized. The film measurements are in better agreement with the digital jaw settings, yielding a difference of <1.6 mm, whereas the EPIDs over-estimated the size of the light field by up to 1.8 mm.

The EPID-based quality assurance technique discussed in this study is a relatively fast and reliable method for checking light radiation congruence. The results presented in (Table 1) suggest that the EPID-based technique is comparable to film, with discrepancies in the order of a fraction of a millimeter (p -value >0.2).

Table 1: The errors for light and radiation field congruence based on electronic portal images and films measurements for An Elekta Precise accelerator with an iViewGT amorphous silicon flat panel imaging system.

	Top (mm)	Bottom (mm)	Left (mm)	Right (mm)	ΔX (mm)	ΔY (mm)
EPID 6MV	1.0	0.8	-1.7	0.0	1.7	1.8
Film 6MV	1.2	1.0	-0.9	-0.8	1.6	1.2

Table 2: A summary of the difference between the digital collimator setting for an acquired portal image and the light field defined on film and EPIDs. The ΔX and ΔY values for films and EPIDs are compared and the respective p -values are listed.

	ΔX (mm)	p -value	ΔY (mm)	p -value
EPID 6MV	1.7		1.8	
		0.72		0.20
Film 6MV	1.6		1.2	

No big difference was observed in the measured size of the light field between films and EPIDs. This is in agreement with J. I. Prisciandaro et al¹⁴. The size of the light field measured with film and EPID was comparable to the digital collimator settings. At most, a 1.8 mm discrepancy was observed in-plane (ΔY).

II. Determination of leaf position accuracy as a QA of dynamic multi-leaf collimator (DMLC) treatment:

The dose profiles obtained by film and EPID are illustrated in (Figure 4.B), cutting through the central cross section along the x axis. Notice that the peak

values and locations of the profiles compare very well with each other. The valleys of the film’s dose profile appear higher than EPID’s, possibly due to the film being more sensitive to low energy scatter. In the profile, the difference of the detector response in the valley region does not affect the present analysis. From (Table 3-A) it is clear that the EPID is able to track the location of individual dose peaks for all the leaf pairs consistently to a standard deviations of 0.12 to 0.47 mm, slightly better than that of 1.00 to 1.26 mm for the Film with buildup. As for the accuracy of peak location, (Table 3-B) shows that film with buildup and EPID track the distance between peaks with a mean of 49.8 and 49.53 mm, respectively and a standard deviation of 0.3 and 1.02 mm, respectively.

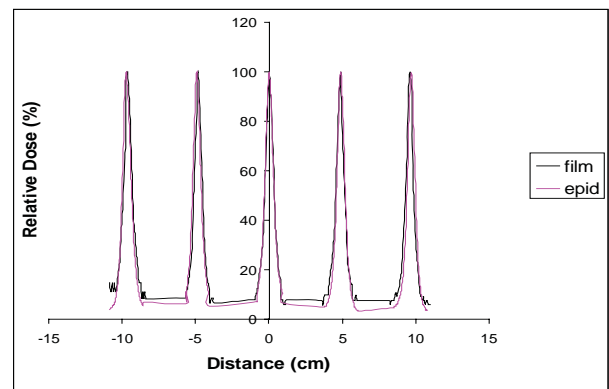


Figure 4 B: Profiles of the central cross-section along the x-axis of the normal test pattern for DMLC QA, acquired using Kodak X Omat film with buildup.

Table 3: Statistical analysis of (A) peak location and (B) interpeak distance for dose profiles using film and EPID. Both peak location and inter-peak distance are measured in millimeter.

	EPID		Film	
	Mean (mm)	SD	Mean (mm)	SD
(A)				
Peak (-10,0)5	98.2	0.25	99.2	1.04
Peak (-05,0)4	49.4	0.47	49.8	1.26
Peak (0,0)1	0.0	0.00	0.0	1.00
Peak (+5,0)2	51.0	0.12	50.0	1.00
Peak (+10,0)3	99.9	0.12	100.0	1.00
(B)				
Peaks 1-2	51		50.0	
Peaks 2-3	48.9		50.0	
Peaks 1-4	49.4		49.8	
Peaks 4-5	48.8		49.4	
Mean	49.53		49.80	
S.D.	1.02		0.3	

Table 4 shows (A) dose peak values and (B) band gaps for all the leaf pairs of the test pattern using film and EPID. (Table 4) shows how EPID is able to track the dose peaks and interband distance of the test pattern compared to those using film with buildup. Note that the true distance between the peaks is 50 mm and these values in (Table 4-A) were normalized to produce the same mean value as film. It is noticed that the dispersion of the dose peak values of EPID is similar to film with buildup, with a standard deviation of 1.59 and 2.41, respectively. In terms of band gap, the average FWHM value of the EPID is similar to film. The values are very consistent, with a mean of 6.34 mm and a standard deviation of 0.34 mm for the EPID, 6.18 and 0.35 mm for the film.

Table 4: (A) Relative dose and (B) FWHM of each peak. Film with 1cm PMMA buildup. The relative dose has no unit, and the FWHM is measured in millimeter

	EPID		Film	
	Mean (mm)	SD	Mean (mm)	SD
(A)				
Peak (-10,0)5	96.6	0.40	94.5	0.41
Peak (-05,0)4	99.0	0.40	94.9	0.42
Peak (0,0)1	100.0	0.51	100.0	0.49
Peak (+5,0)2	96.9	0.45	98.0	0.47
Peak (+10,0)3	96.6	0.40	95.1	0.42
Mean	97.9		96.5	
SD	1.59		2.41	
(B)				
Peak (-10,0)5	6.60	0.32	6.40	0.35
Peak (-05,0)4	6.40	0.29	6.20	0.17
Peak (0,0)1	6.70	0.09	6.60	0.16
Peak (+5,0)2	6.10	0.21	6.00	0.21
Peak (+10,0)3	5.90	0.20	5.70	0.15
Mean	6.34		6.18	
SD	0.34		0.35	

In this study, the feasibility of using an EPID as an alternative to film for routine DMLC QA was investigated. Four measures—peak location, interpeak distance, gap width and peak value—of the test pattern of this study were used to evaluate the consistency of DMLC motion and output (peak value). Mean and standard deviation (SD) of each measure were calculated to determine the normal range for that measure. Generally, a smaller (SD) means tighter normal range and indicates that the detector is more sensitive. From the test results of each measure tabulated in (Tables 3 and 4), the sensitivity of EPID is comparable to that of film for this QA procedure.

The standard deviation of the FWHM for EPID is ± 0.34 from the mean FWHM, smaller than ± 0.35 for film. If $\text{mean} \pm 2\text{SD}$ is the range for normal FWHM, then EPID has a slightly tighter tolerance than the film to determine whether the gap of the test pattern is problematic. An additional advantage of using EPID for this QA procedure is that absolute peak positions can be easily checked with EPID, which is hard to perform with film.

CONCLUSION

In this study, the use of an EPID for light and radiation field congruence tests was examined. The results indicate that the EPID-based procedure is comparable to film. Both the film and EPID-based light and radiation field congruence techniques have been shown to be sensitive to below the allowed 2 mm or 1% discrepancy on each side of the square field. Considering the additional time to setup and process film, the EPID-based technique is a fast and reliable alternative. With the growing desire to implement EPID for IMRT quality assurance, integrating EPIDs into conventional radiation therapy QA is an important first step.

Finally, all the analysis performed in the study require images in digital format. The EPID image is digital intrinsically; the film, on the other hand, is analog. To digitize a film requires significant time and manpower, making it very tedious to perform frequently and routinely. Without a digitized image, we can only visually inspect the film, a procedure which is subjective and not always reliable. Since we have demonstrated in this study that an EPID is as sensitive QA tool as film for our routine DMLC QA procedure, it is concluded that film can be replaced by an EPID for this procedures.

ACKNOWLEDGMENTS

Two of the authors (M. A. A.) and (W. F. M.) acknowledge the support from department of Oncology and Nuclear Medicine, Kasr Al-Ainy Hospital, Cairo University where the work was completed and prepared.

REFERENCES

1. Ploeger LS, Smitsmans MH, Gilhuijs KG, van Herk M. Accurate measurement of the dynamic response of a scanning electronic portal imaging device. *Med.Phys.* 2001 Mar;28(3):310-6.
2. Pasma KL, Dirx ML, Kroonwijk M, Visser AG, Heijmen BJ. Dosimetric verification of intensity modulated beams produced with dynamic multileaf collimation using an electronic portal imaging device. *Med.Phys.* 1999 Nov;26(11):2373-8.
3. Chang J, Ling CC. Using the frame averaging of aS500 EPID for IMRT verification. *J.Appl.Clin.Med.Phys.* 2003 Autumn;4(4):287-99.
4. Munro P, Bouius DC. X-ray quantum limited portal imaging using amorphous silicon flat-panel arrays. *Med. Phys.* 1998 May;25(5):689-702.

5. Samant SS, Zheng W, Parra NA, Chandler J, Gopal A, Wu J, et al. Verification of multileaf collimator leaf positions using an electronic portal imaging device. *Med.Phys.* 2002 Dec;29(12):2900-12.
6. Sonke JJ, Ploeger LS, Brand B, Smitsmans MH, van Herk M. Leaf trajectory verification during dynamic intensity modulated radiotherapy using an amorphous silicon flat panel imager. *Med.Phys.* 2004 Feb;31(2):389-95.
7. Chang J, Mageras GS, Chui CS, Ling CC, Lutz W. Relative profile and dose verification of intensity-modulated radiation therapy. *Int.J.Radiat.Oncol.Biol.Phys.* 2000 Apr 1;47(1):231-40.
8. Warkentin B, Steciw S, Rathee S, Fallone BG. Dosimetric IMRT verification with a flat-panel EPID. *Med.Phys.* 2003 Dec;30(12):3143-55.
9. Burman C, Chui CS, Kutcher G, Leibel S, Zelefsky M, LoSasso T, et al. Planning, delivery and quality assurance of intensity-modulated radiotherapy using dynamic multileaf collimator: A strategy for large-scale implementation for the treatment of carcinoma of the prostate. *Int.J.Radiat. Oncol.Biol.Phys.* 1997 Nov 1;39(4):863-73.
10. Ling CC, Burman C, Chui CS, Kutcher GJ, Leibel SA, LoSasso T, et al. Conformal radiation treatment of prostate cancer using inversely-planned intensity-modulated photon beams produced with dynamic multileaf collimation. *Int.J.Radiat.Oncol.Biol.Phys.* 1996 Jul 1;35(4):721-30.
11. LoSasso T, Chui CS, Ling CC. Physical and dosimetric aspects of a multileaf collimation system used in the dynamic mode for implementing intensity modulated radiotherapy. *Med.Phys.* 1998 Oct;25(10):1919-27.
12. LoSasso T, Chui CS, Ling CC. Comprehensive quality assurance for the delivery of intensity modulated radiotherapy with a multileaf collimator used in the dynamic mode. *Med.Phys.* 2001 Nov;28(11):2209-19.
13. LoSasso TJ. Quality assurance of IMRT. In: Fuks Z, Leibel SA, Ling CC, editors. *A practical guide to intensity-modulated radiation therapy* Madison: Medical Physics Publishing; 2003. pp. 147-67.
14. Prisciandaro JI, Herman MG, Kruse JJ. Utilizing an electronic portal imaging device to monitor light and radiation field congruence. *J.Appl.Clin.Med.Phys.* 2003 Autumn;4(4):315-20.
15. Langmack KA. Portal imaging. *Br.J.Radiol.* 2001 Sep;74(885):789-804.